Feasibility investigations for vibration-based remote scour monitoring of railway bridges

Kazuhiro Yoshitome
Master Student, Dept. of Civil & Earth Resources Engineering, Graduate School of Engineering, Kyoto University, Kyoto, Japan

Chul-Woo Kim,
Professor, Dept. of Civil & Earth Resources Engineering, Graduate School of Engineering, Kyoto University, Kyoto, Japan

Masaki Shinoda
Senior chief expert, Fuji Electric Co. Ltd., Tokyo, Japan

Shinji Kitagawa
Assistant manager, Fuji Electric Co. Ltd., Tokyo, Japan

Masahiro Kondo
Manager, West Japan Railway Company, Osaka, Japan

Siu-Kui Au
Professor, Dept. of Civil Engineering and Industrial Design, The University of Liverpool, Liverpool, UK

ABSTRACT: This study investigates feasibility of vibration-based scour monitoring as an alternative method for the impact test. A wireless sensing device was adopted for the long-term monitoring which can be remotely controlled. The target bridge was reinforced against scouring after the long-term scour monitoring. This study examines the feasibility of scour detection by comparing the vibration characteristics of the piers before and after the reinforcement. Observations for the bridge pier before reinforcement demonstrated that the probability distribution of dominant frequencies under higher water level during flood of the pier showed clearly different pattern to those under lower water level. On the other hand, those probability distributions of dominant frequencies of the reinforced pier showed constant pattern despite of the water level

1. INTRODUCTION

Scouring is the erosion of the riverbed caused by fluctuation in the flow of river, turbulence, etc. If scouring occurs around the foundation ground, the substructure may settle, incline, or fall. Since the deformation in substructure also affects the superstructure, the trains should be prohibited to pass on the bridges with the scoured substructures. Also, fatal accidents possibly occur if train forcedly passes over the scoured bridges.

The impact test on the railway bridge pier to identify changes in frequencies has been adopted as a promising scour detection method in Japan. However, the impact test is a laborious and time-consuming method, and is inapplicable for the real time monitoring to make a proper decision on the train operation control during heavy rains. Therefore, a remote monitoring system and a decision rule to detect scouring are desired.

This study aims to propose how to judge the soundness of the piers efficiently and quantitatively without approaching the bridge piers. As scouring countermeasure, the target pier and the foundation around the pier is reinforced by concrete. To investigate the feasibility of the

proposed method, this study indirectly examines the possibility of scour detection by comparing the vibration characteristics of the piers before and after the reinforcement against scouring on assumption that scouring is likely to occur before the reinforcement and scouring after the reinforcement does not occur.

2. METHODOLOGY

In this paper, two types of identification methods, stochastic subspace identification (SSI) and Bayesian operational modal analysis (BAYOMA) are used.

2.1. Stochastic Subspace Identification

The dynamical system is modeled as the following state space model (Heylen et al. 1997, van Overschee and de Moor 1993 and 1996, Goi et al. 2016).

$$\mathbf{x}(k+1) = A\mathbf{x}(k) + \mathbf{w}(k) \tag{1}$$
$$\mathbf{y}(k) = \mathbf{C}\mathbf{x}(k) + \mathbf{v}(k)$$

Therein, $\mathbf{x}(k)$ and $\mathbf{y}(k)$ respectively denote the state of structure and measurement at each time step k. Also, $\mathbf{w}(k)$ and $\mathbf{v}(k)$ respectively denote the process noise and measurement noise vectors. They are assumed to be stationary white noise. System matrices $\mathbf{A}$ and $\mathbf{C}$, which contain the modal information, are estimated using least-squares method for the minimal prediction error of state $\mathbf{x}(k)$ given by the forward Kalman filter. The poles of the dynamical system provide modal properties of the dynamical system.

The algorithm for the SSI is described briefly. First, we obtain the projection matrix $\boldsymbol{O}_i$, as estimated from Eq. (2).

$$\boldsymbol{O}_i = \mathbf{Y}_f \mathbf{Y}_p^T \left(\mathbf{Y}_p \mathbf{Y}_p^T\right)^{\dagger} \mathbf{Y}_p \tag{2}$$

There, $(\cdot)^{\dagger}$ denotes the Moore-Penrose pseudo-inverse matrix. $\mathbf{Y}_f$ and $\mathbf{Y}_p$ represent the block Hankel matrices of the future and past outputs as shown in Eq. (3) and Eq. (4).

$$\tag{3}$$

$$\mathbf{Y}_p = \begin{bmatrix} \mathbf{y}(0) & \mathbf{y}(1) & \dots & \mathbf{y}(j-1) \\ \dots & \dots & \dots & \dots \\ \mathbf{y}(i-2) & \mathbf{y}(i-1) & \dots & \mathbf{y}(i+j-3) \\ \mathbf{y}(i-1) & \mathbf{y}(i) & \dots & \mathbf{y}(i+j-2) \end{bmatrix}$$

$$\mathbf{Y}_f = \begin{bmatrix} \mathbf{y}(i) & \mathbf{y}(i+1) & \dots & \mathbf{y}(i+j-1) \\ \dots & \dots & \dots & \dots \\ \mathbf{y}(2i-2) & \mathbf{y}(2i-1) & \dots & \mathbf{y}(2i+j-3) \\ \mathbf{y}(2i-1) & \mathbf{y}(2i) & \dots & \mathbf{y}(2i+j-2) \end{bmatrix} \tag{4}$$

The singular value decomposition (SVD) is then applied to factorize $\boldsymbol{O}_i$ as shown below.

$$\boldsymbol{O}_i = \mathbf{U}\mathbf{S}\mathbf{V}^T \simeq (\mathbf{U}_1 \mathbf{U}_2)\begin{pmatrix} \mathbf{S}_1 & \mathbf{0} \\ \mathbf{0} & \mathbf{0} \end{pmatrix}(\mathbf{V}_1 \mathbf{V}_2)^T = \mathbf{U}_1 \mathbf{S}_1 \mathbf{V}_1^T \tag{5}$$

In those equations, $\mathbf{U}$ and $\mathbf{V}$ are unitary matrices with an appropriate size; $\mathbf{S}$ is a diagonal matrix with non-negative elements. Diagonal elements of $\mathbf{S}$ are known as singular values of $\boldsymbol{O}_i$. Singular values in $\mathbf{S}$ are listed in descending order. Therefore, the components in $\mathbf{U}_1 \mathbf{S}_1 \mathbf{V}_1^T$ include most of the information defining the elements in $\boldsymbol{O}_i$. Components in $\mathbf{U}_2 \mathbf{S}_2 \mathbf{V}_2^T$ are regarded as trivial components. The optimal state sequence predicted by the Kalman filter in a least squares sense is obtained as shown below.

$$\mathbf{X}_i = \mathbf{S}_1^{1/2} \mathbf{V}_1^T \tag{6}$$

where $\mathbf{X}_i = [\mathbf{x}(i) \quad \mathbf{x}(i+1) \quad \dots \quad \mathbf{x}(i+j-1)]$.

The system matrices are obtainable from $\mathbf{X}_i$. The number of poles corresponds to the number of singular values determined in Eq. (5). In other words, we can extract the modal response of the bridge from the measured acceleration data by the SVD.

2.2. Bayesian Operational Modal Analysis

The data consists of digital acceleration time history at a limited number of measurements on the subject structure, denoted by $D = \ddot{\mathbf{x}}_j \in R^n$ ($j = 1, \dots, N$), where n denotes measured degrees of freedom and N is the number of samples per measurement channel. Assuming classical

damping, the data can be represented as shown in Eq. (8).

$$\ddot{x}_j = \sum_{i=1}^{m} \boldsymbol{\phi}_i \, \ddot{\eta}_i(t_j) + \boldsymbol{\epsilon}_j \qquad (7)$$

where the sum is over all contributing modes; $\boldsymbol{\epsilon}_j$ is the prediction error; $\boldsymbol{\phi}_i \in R^n$ is the mode shape confined to the measured dofs; $\eta_i(t)$ is the ith modal response satisfying the uncoupled modal equation

$$\ddot{\eta}_i(t) + 2\zeta_i\omega_i\dot{\eta}_i(t) + \omega_i^2\eta_i(t) = p_i(t) \qquad (8)$$

where ω_i, ζ_i, p_i are the natural angular frequency, damping ratio and modal force, respectively. θ consists of the natural frequency, damping ratio and mode shape of the modes of interest. Other parameters to be discussed later.

A Bayesian formulation based on the Fast Fourier Transform first appeared. (Yuen and Katafygiotis 2003) Fast algorithms that allow practical implementation have been recently developed. (Au 2011) Specifically, the data is represented in terms of its FFT, i.e., $D = \{F_k\}$, where

$$F_k = \sqrt{\frac{2\Delta t}{N}} \sum_{j=1}^{N} \ddot{x}_j \exp\left[-\frac{2\pi \mathbf{i}(k-1)(j-1)}{N}\right] \qquad (9)$$

with Δt is the sampling interval. For $k = 2,3,\dots N_q$, the FFT corresponds to frequency $f_k = (k-1)/N\Delta t$, where $N_q(= N/2 + 1)$ is the frequency index at the Nyquist frequency. If the FFTs in the full bandwidth are used, the representations in terms of time-domain data or frequency-domain data are equivalent because they are related by an invertible transformation.

In the frequency-domain approach, determining the likelihood function requires deriving the probability distribution of the FFT data for given θ. Elegant results can be obtained for sufficiently high sampling rate and long data duration often encountered in practice. In this case, as a standard result in spectral analysis

(Schoukens and Pintelon 1991), the FFTs at different frequencies are asymptotically independent. The real and imaginary parts of F_k are jointly Gaussian with zero mean and a covariance matrix given by

$$\mathbf{C}_k = \frac{1}{2}\begin{bmatrix} \boldsymbol{\Phi}\mathrm{Re}\,\mathbf{H}_k\boldsymbol{\Phi}^{\mathrm{T}} & -\boldsymbol{\Phi}\mathrm{Im}\,\mathbf{H}_k\boldsymbol{\Phi}^{\mathrm{T}} \\ \boldsymbol{\Phi}\mathrm{Im}\,\mathbf{H}_k\boldsymbol{\Phi}^{\mathrm{T}} & \boldsymbol{\Phi}\mathrm{Re}\,\mathbf{H}_k\boldsymbol{\Phi}^{\mathrm{T}} \end{bmatrix} + \frac{S_e}{2}\mathbf{I}_{2n} \qquad (10)$$

where $\boldsymbol{\Phi} = [\boldsymbol{\phi}_1, \boldsymbol{\phi}_2, \dots, \boldsymbol{\phi}_m] \in R^{n \times m}$; S_e is the spectral density of the prediction error; $\mathbf{I}_{2n}$ denotes the 2n×2n identity matrix; and *Im* and *Re* denote the real and imaginary parts, respectively; $\mathbf{H}_k \in C^{m \times m}$ is the theoretical spectral density matrix of the modal acceleration responses and is given by Eq. (11).

$$\mathbf{H}_k = \mathrm{diag}(\boldsymbol{h}_k)\,\mathbf{S}\,\mathrm{diag}(\boldsymbol{h}_k^*) \qquad (11)$$

Here $\mathbf{S} \in C^{m \times m}$ is the spectral density matrix of modal forces; $diag(\cdot)$ denotes a diagonal matrix with the ith diagonal element equal to h_{ik} ; an asterisk denotes a conjugate transpose; $\boldsymbol{h}_k \in C^m$ is a vector of modal transfer functions with the element equal to

$$h_{ik} = \left[(\beta_{ik}^2 - 1) + \mathbf{i}(2\zeta_i\beta_{ik})\right]^{-1} \qquad (12)$$

where, $\beta_{ik} = f_i/f_k$ is a frequency ratio.

Using the above result for the likelihood function and adopting a uniform prior distribution, the resulting posterior PDF is given by Eq. (13).

$$p(\theta|\{D, M\}) \propto \exp[-L(\theta)] \qquad (13)$$

where $L(\theta)$ is the NLLF (negative log-likelihood function) given by Eq. (14).

$$L(\theta) = \frac{1}{2}\sum_k \ln|\mathbf{C}_k(\theta)| + \frac{1}{2}\sum_k \boldsymbol{Z}_k^T \mathbf{C}_k(\theta)^{-1}\boldsymbol{Z}_k \qquad (14)$$

where, $\boldsymbol{Z}_k$ contains the real and imaginary part of F_k. The sums in Eq. (14) indicate summation of all frequencies in the selected frequency band only. Here, the set of modal parameters θ consists of the natural frequencies f_i, damping ratios ζ_i, mode shape matrix $\boldsymbol{\phi}_i$, PSD matrix **S** of modal forces and PSD S_e of the prediction error for the modes of interest in the selected band.

3. TARGET BRIDGE AND MONITORING INFORMATION

The target bridge was constructed more than 100 years ago. It is a double railway track steel plate girder bridge, and mass of the girder is around 30 t. Two lanes are connected on the superstructure, but two RC piers support each lane independently. Height of pier is 5.45m and width is 3.96m. As there was high potential risk of scouring on the target piers, the long-term scour monitoring was carried out.

The elevation view of the target pier is shown in Figure 1. Shaded part in red around the pier indicates the range reinforced by concrete. The foundation is also reinforced by concrete for scouring. A wireless 3-axis accelerometer was installed on the center of top of the bridge pier. The sampling frequency of the measurement was 200Hz. Impact hammer test was conducted in 2001, and natural frequency of the bridge pier before the reinforcement was 15.93 Hz. Figure 2 shows the photos of the target bridge piers before and after the scouring reinforcement.

4. PRELIMINARY INVESTIGATION

To identify the modal properties of the bridge pier excited by a passing train, this study utilizes SSI and stability criteria (SC) that extracts locally stable vibration modes (Chang and Kim, 2016). Figure 3 shows the acceleration sensor deploying map. Figure 4 shows SD in which the horizontal and vertical axis respectively stand for the estimated frequencies and the model order that required in the SSI procedure (described in chapter 2). The black dots show the modal frequencies estimated from each of the model orders. The red circles indicate stably estimated modes that satisfies predefined deviation

tolerances of the modal properties (the natural frequencies, damping ratio, and mode shapes).

This study adopted the frequency deviation tolerance as 0.25 Hz, the damping deviation tolerance as 0.1 %, and the lower bound of Modal Assurance Criteria (MAC) as 0.95. The vertical blue broken lines show predominant modes that appear stably throughout a wide range of model order and satisfy the deviation tolerances.
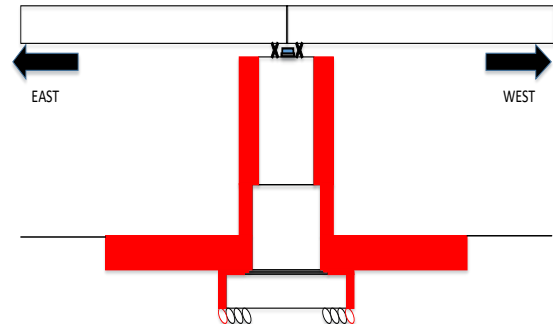

Figure 1: Elevation view of the target pier.

(a)   Before repair

(b)   After reinforcement
Figure 2: Photos of target bridge piers.

The predominant frequencies were identified at 4.81 Hz, 9.35 Hz, 10.54 Hz, 14.73 Hz, 15.39 Hz, 20.01 Hz and 29.34 Hz. Fig.5 shows the mode shape relevant to 15Hz. This frequency corresponds to the natural frequency estimated from the impact hammer test before the reinforcement. As shown in Fig.5, this mode shape is relevant to the transversal rocking mode of the pier.

5. COMPARISON OF POWER SPECTRAL DENSITY

Figure 6 shows the power spectral density (PSD) curves of the lateral acceleration estimated from ambient vibration during flood. The red and blue lines respectively stand for the PSDs before and after reinforcement for scouring. We focus on 15Hz, which is the frequency of the bridge pier's rocking mode before reinforcements. This PSD curve demonstrates that the power around 15Hz is decreased after scouring reinforcement. This indicates that the rocking vibration of the bridge pier (shown Figure 5) is suppressed by the reinforcement.

6. BAYESIAN MODAL IDENTIFICATION

The Bayesian modal identification is applied to improve accuracy of modal identification using ambient vibration. In Bayesian modal identification, it is necessary to determine the frequency band for the FFT. In this research, we apply for the range from 14Hz to 17Hz so as to cover the frequency around 15 Hz, which is relevant to the rocking mode of bridge pier before the reinforcement. The frequency band of the pier after the reinforcement was determined according to the natural frequency before the reinforcement. However, if the natural frequency of the bridge pier greatly changes after the reinforcement, the target range must be changed.

BAYOMA was applied to acceleration data in three axial directions. Figure 7 and Figure 8 show the histograms of the identified frequencies under normal and flood conditions, where 'the flood condition' represents the condition such that the distance between the bridge girder and the water surface is 2.5m or less and the operation is suspended. Figure 7 shows the result before the reinforcement, Figure 8 shows the result after the reinforcement. According to Figure 7, identified frequencies appear around 16.4Hz and around 14.5Hz under the normal condition, whereas they dominantly appear around 15.7Hz in the flood condition. This observation suggests that the vibration characteristics greatly change between the normal and flood condition before the reinforcement. The natural frequency of the bridge pier is susceptible to river flow. In Figure 8, however, the identified frequencies are not likely to be identified around 16.4Hz and 15.7Hz but they appear around 14.5Hz.
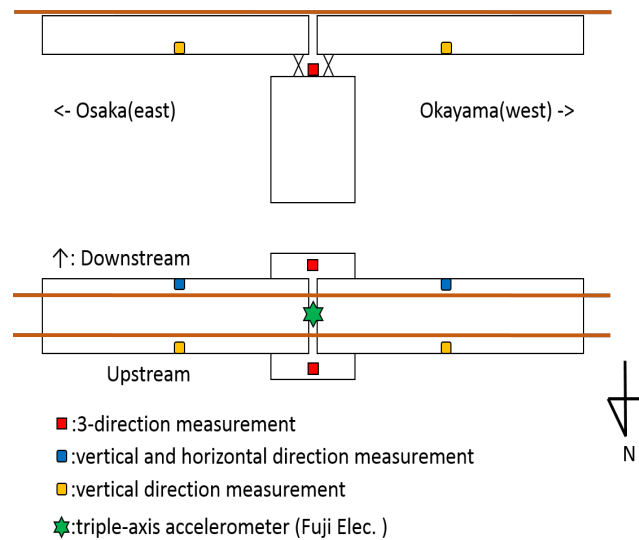

■ :3-direction measurement
■ :vertical and horizontal direction measurement
■ :vertical direction measurement
★ :triple-axis accelerometer (Fuji Elec.)

Figure 3: Elevation view and plan view of the acceleration sensor installation position.
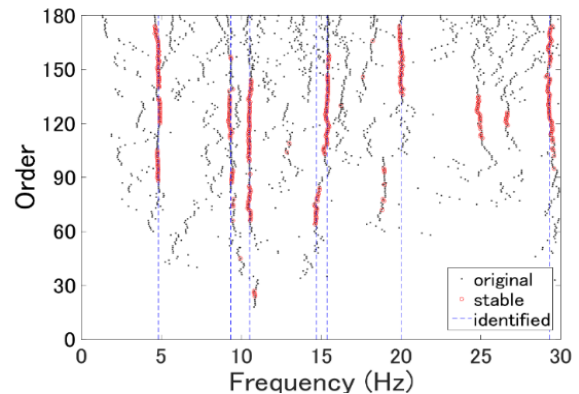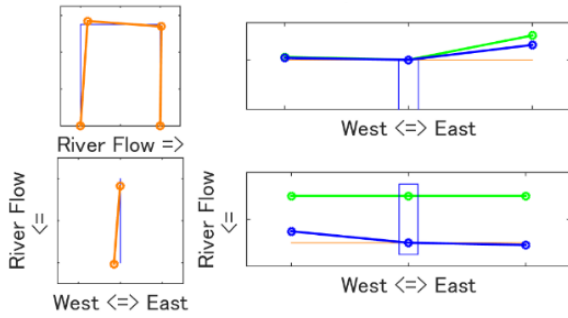

Figure 4: Stabilization Diagram (SD).

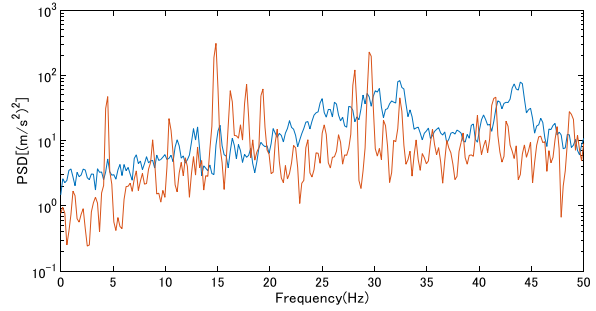*Figure 5: Identified mode shape (15.39Hz).*

Figure 6: PSD of the acceleration installed on the pier during flood condition before and after reinforcements (Blue: before reinforcement, Red dotted line: after reinforcement).
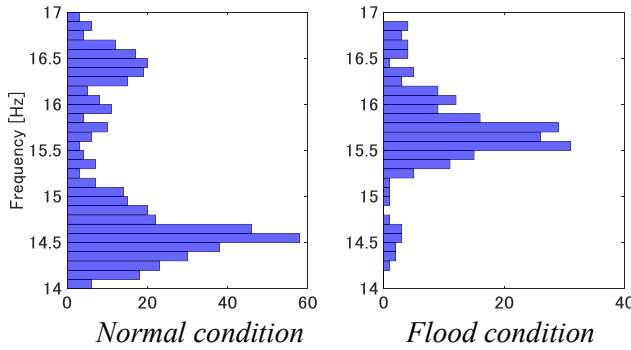

Normal condition   Flood condition

Figure 7: Identification frequencies of 14 to 17Hz (three directions, before reinforcement).

Normal condition   Flood condition
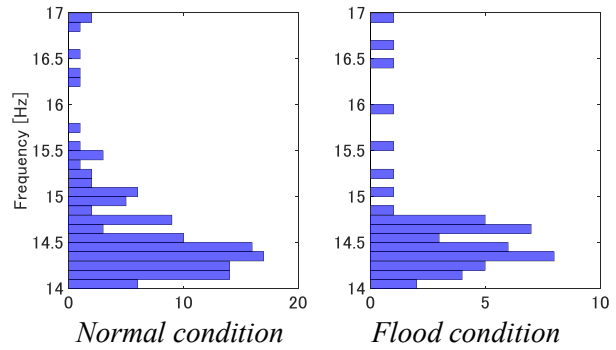
Figure 8: Identification frequencies of 14 to 17Hz (three directions, after reinforcement).

Normal condition   Flood condition
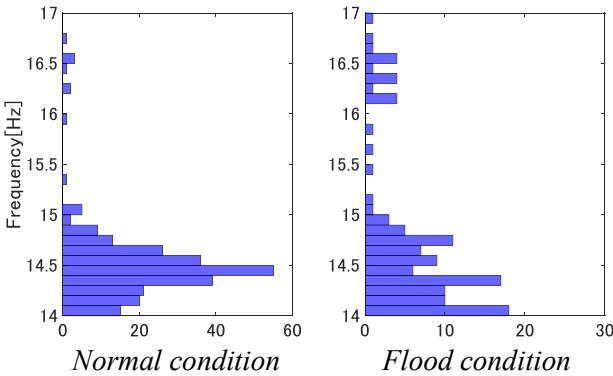
Figure 9: Identification frequencies of 14 to 17Hz (longitudinal direction, before reinforcement).

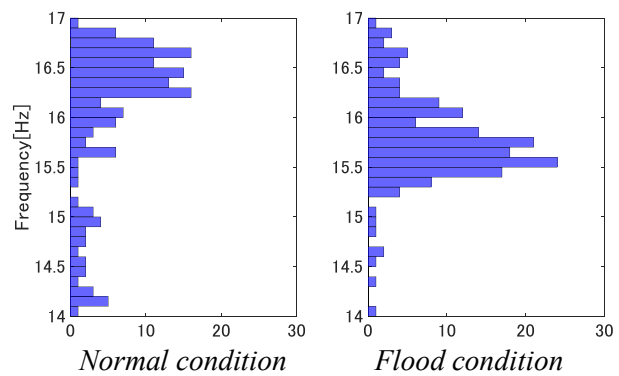Normal condition   Flood condition

Figure 10: Identification frequencies of 14 to 17Hz (transversal direction, before reinforcement).

According to Figure 7, identified frequencies appear around 16.4Hz and around 14.5Hz under the normal condition. Similar analysis using uniaxial data was considered in order to investigate causes behind these two prominences. Figure 9 and Figure 10 show the histograms of the identified frequencies under normal and flood conditions before the reinforcement in which Figure 9 shows the result by using vibration data in the longitudinal direction, and Figure 10 shows those in the transversal direction. Figure 9 demonstrates identified frequencies around 14.5 Hz is due to vibration in the

longitudinal direction. Figure 10 demonstrates identified frequencies around 16.4Hz is due to vibration in the transverse direction.

It is noteworthy that the identified frequency in transversal direction decreased due to the rise of the water level as shown in Figure 10.

7. CONCLUSIONS

The following two observations were given through the remote ambient vibration monitoring.

1. Comparing the PSDs of the ambient vibration data before and after the pier scour reinforcement, the power of the PSD after the reinforcement of the piers is decreased. It demonstrates that the rocking vibration of the bridge piers is suppressed after the reinforcement.

2. Before the reinforcement, vibration characteristics of the pier significantly varied between the normal condition and the flood condition. Especially the natural frequency of the pier in transversal direction decreased due to the increase in water level. However, after the reinforcement, the vibration characteristics hardly change between the normal condition and the flood condition.

It was found that the vibration characteristics greatly changed before and after reinforcement. Further studies are needed to link vibration characteristics changes to the severity of the scouring.

REFERENCES

Au SK. (2011) 'Fast Bayesian FFT method for ambient modal identification with separated modes' J Eng Mech ASCE, 137(3):214-26

Au, S.K., Zhang, F.L. and Ni, Y.C. (2013), 'Bayesian operational modal analysis: theory, computation, practice'. Computers & Structures, 126: 3-14.

Chang, K.C. and Kim, C.W. (2016), "Modal-parameter identification and vibration-based damage detection of a damaged steel truss bridge", Engineering Structures, 122: 156-173.

Goi, Y. and Kim, C.W. (2016), "Mode identifiability of a multi-span cable-stayed bridge utilizing stabilization diagram and singular values", Smart Structures and Systems, An Int J., 17(3): 391-411.

Heylen, W., Lammens, S. and Sas, P. (1997), "Modal Analysis Theory and Testing", K.U. Leuven, Belgium.

Kim, C.W. Kitauchi, S., Sugiura, K., Kawatani, M., and Kai, M. (2013), 'Structural damage detection of a multi-span continuous steel-truss bridge focusing on traffic vibration', J. JSCE A1, 69(3): 557-571.

Koruk H, Sanliturk KY (2011) 'Damping uncertainty due to noise and exponential windowing' J Sound Vib., 330(23): 5690-706

Lutes DL, Sarkani S. (1997) 'Stochastic analysis of structural and mechanical vibrations' New Jersey, Prentice Hall

Schoukens J., Pintelon R. (1991) 'Identification of linear systems' a practical guideline for accurate modeling, London: Pergamon Press

van Overschee, P. and de Moor, B (1996), "Subspace Identification for Linear Systems", Kluwer Academic Publishers.

van Overschee and de Moor (1993), "Subspace algorithms for the stochastic identification problem", Automatica, 29(3): 649-660.

Yuen KV, Kuok SC (2011) 'Bayesian methods for updating dynamic models' Appl Mech Rev, 64(1): 010802-1-010802-18

Yuen KV, Katafygiotis LS (2003) 'Bayesian Fast Fourier Transform approach for modal updating using ambient data' Adv Struct Eng., 6(2):81-95